Volume 1 | Number 1 | Jan 2013 | Pages 1–100

Journal of
Materials Chemistry A

Materials for energy and sustainability
www.rsc.org/materialsA

Li⁺

ROYAL SOCIETY
OF CHEMISTRY

ROYAL SOCIETY
OF CHEMISTRY

www.rsc.org/materialsA

ARTICLE TYPE

Rapid Microwave-assisted Green Production of Crystalline Polyimide for Enhanced Visible-Light-Induced Photocatalytic Hydrogen Production

Li Lin,[a] Ping Ye,[a] Chang Cao,[a] Qi Jin,[a] Geng-Sheng Xu,[a] Yu-Hua Shen,[a, b] and Yu-Peng Yuan*[a, b]

Herein we used a rapid "microwave (MW)-assisted heating synthesis" to produce the crystalline polyimide in minutes. Importantly, the present strategy avoids the tedious washing
10 **process for the produced polyimide. Benefiting from the relatively high crystalline, the obtained polyimide shows improved photocatalytic H_2 production under visible light irradiation.**

Photocatalytic hydrogen production through water reduction has
15 great potential to provide renewable and clean hydrogen energy in the future. In the last several decades, tremendous efforts have been paid on developing various photocatalysts to produce hydrogen fuels through solar water splitting.[1-3] So far, over one hundred materials have been demonstrated as promising
20 photocatalysts for hydrogen production under UV and visible light irradiation.[4] Nevertheless, these developed photocatalysts are always the metal-containing semiconductors that would now only raise the economic cost in terms of large-scale production but also the metal ion contamination concerns. In comparison,
25 carbon based semiconductors could be the excellent candidates owing to their chemical stability and "earth-abundant" nature.
More recently, polymeric photocatalyst, graphitic carbon nitride (g-C_3N_4), for hydrogen production has received tremendous attention.[5, 6] Unlike the metal-containing photocatalysts that
30 would raise the economic cost for large-scale application, g-C_3N_4 was composed of earth-abundant C and N element. Moreover, this metal-free photocatalyst holds high thermal and chemical stability, and has small band gap for visible light response with suitable band edge levels for water splitting.[5] However, the
35 photocatalytic water splitting efficiency of g-C_3N_4 is not high enough for practical applications. Therefore, developing new polymeric photocatalysts are still great interest in photocatalysis research. Crystalline polyimides (PIs) were reported for photocatalytic hydrogen production using visible light.[7-9]
40 Polyimides are polymers of imide monomers and have been widely used in the electronics industry, separation, and aerospace due to their excellent thermal and chemical stability.[10] Presently, the synthesis of PIs usually requires the tedious procedures or high temperature with long reaction time (several hours at least).
45 For example, PIs can be produced through the polymerization of amines and anhydride in cresol or N-methylpyrrolidone solvents. However, azeotropic distillation using toxic organic solvent, such as xylene, is always involved to promote the polymerization process, making the procedure for PIs production not only tedious
50 but also not environmentally-friendly.[11, 12] Zou *et al* reported an organic-solvent-free process through heating melamine and pyromellitic dianhydride (PMDA) in air at 325 °C for 4 h, which is still time- and energy consuming process.[5] Our group recently reported a rapid microwave-ionothermal process for PIs
55 production, in which $ZnCl_2$ was used as microwave absorber. This strategy allows the PIs to be produced within 3 mins. Unfortunately, the following tedious wash process with HCl makes the strategy not environmental-benign.[13]
Herein we report a facile and rapid synthesis of PIs using our
60 recently developed "microwave (MW)-assisted heating synthesis" strategy.[14] It has been revealed that, for PI synthesis, the heating temperature should be over 560 K (the melting point of PMDA) to ensure the complete reaction of melamine and PMDA.[5] In MW-assisted heating strategy, the CuO as the MW-
65 absorber can raise the temperature up to 1285 K within 7 min.[15] Therefore, MW-assisted method can ensure the high temperature for complete polymerization reaction between melamine and PMDA. In addition, this strategy not only allows the production of PIs in minutes but also avoids the tedious rinsing process after
70 polymerization of melamine and PMDA. Most importantly, the as-prepared PIs show improved photocatalytic hydrogen production than the one obtained by direct heating melamine and PMDA in air. To our knowledge, this is the first report of MW-assisted synthesis of polyimide photocatalysts.
75 Typically, the obtained products through MW-assisted polymerization of melamine and pyromellitic dianhydride are labeled as MPI$_t$, in which t is the MW heating time (min). A comparison sample of PI was also prepared by heating melamine and pyromellitic dianhydride at 325 °C for 4 h in air (labeled as
80 PI325) according to literature protocols.[7] The model reaction of photocatalytic hydrogen production through proton reduction was used to evaluate the photocatalytic performance of as-prepared PI samples.
The structure and morphology of the obtained products were
85 characterized by powder XRD, FT-IR, N_2 adsorption/desorption,

SEM, and TEM. In comparison to previous synthetic strategies, a distinct priority of present MW-assisted heating synthesis is the very short reaction time. As shown in Fig. 1a, the sample prepared at 700 W MW power for 7 min (MPI$_7$) show several
5 distinct diffraction peaks, revealing the crystalline nature of the products. In addition, the XRD pattern of MPI$_7$ is essentially the same as that of PI325, confirming the PI formation under MW-assisted heating for 7 min. Note that the peak intensities of the MPI$_7$ sample are stronger than those of PI325 sample, indicating
10 an improved crystalline quality of the MPI$_7$ sample. The similar phenomenon was also observed in g-C$_3$N$_4$ synthesis, wherein the diffraction peak intensity of the sample obtained by MW-assisted heating is also stronger than that of the sample produced directly by electric heating.[14] This result could be caused by the MW-
15 enhanced polymerization process that provides stronger localized heating as opposed to bulk thermal treatment. It was found that the molecules with a permanent dipole moment will try to align to the applied electromagnetic field under microwave irradiation, and thus resulting in rotation, friction, and collision of molecules.
20 As a result, the activation of the C-O-C in PMDA can therefore be substituted easier by the amine group in melamine, and thereby promote the polymerization reaction. Meanwhile, the direct heating of the molecules under microwave irradiation causes the very fast and homogeneous heating, which will also
25 accelerate the polymerization process.[16] Normally, the higher the crystalline of a catalyst, the higher the photocatalytic activity. Notably, a wide diffraction peak at 27.5º is resulted from the periodic array of interlayer aromatic packing, as occurs in g-C$_3$N$_4$.[17, 18]

reveals the total imidization of the product. The stronger
40 absorption band at around 3200 cm^{-1} is the –NH$_2$ stretching vibration mode. XRD and FT-IR analysis clearly reveal that the polymerization of melamine and pyromellitic dianhydride into polyimide can be completed in 7 minutes. Note that no further rinsing process is needed to treat the products. To the best of our
45 knowledge, this case is the first example that polyimide can be prepared within such a short time directly.

Typical microscopy of MPI$_7$ sample is illustrated in Fig. 1c. The microscale particles with irregular morphology of resultant PIs were formed. It is worthy noting that lot of macropores are
50 observed within the as-prepared PIs. The formation of macropores should be caused by the gas evolution during polymerization. Interestingly, several ultrathin sheets are formed. To the best of our knowledge, this is the first case of forming PI ultrathin sheets. The detailed mechanism for these ultrathin sheets
55 formation is still not clear at present stage. These ultrathin sheets can be further visualized by TEM observations, as shown in Fig. 1d. Unfortunately, the HRTEM of MPI$_7$ is not attainable due to the polymeric nature of PI sample. The energy-dispersive X-ray spectroscopy (EDS) further reveals that the as-produced sample is
60 mainly composed of C, N, and O elements (Fig.S1).

The band gap energy of the MPI$_7$ sample is determined to be 2.7 eV from the ultraviolet-visible spectrum, which is slightly blue-shift to that of PI325 sample (Eg=2.6 eV) (Fig. S2). The difference in light absorption behaviours should be caused by the
65 various polymerization processes, as revealed by improved crystalline quality. The quantitative elemental analysis for MPI$_7$ shows the following results: C: 47.1%; N: 26.2%; H: 2.4%, and O was calculated to be 24.3%, which is essentially the same as that of PI325 sample: C: 47.9%; N: 27.3%; H: 2.3%. The elemental
70 analysis result is well consistent with the theoretic formula C$_{12}$N$_4$O$_4$H$_2$: C: 54.1%; N: 21.1%; H: 0.8%, and O: 24.1%, as shown by the molecular structure of polyimide (Fig. S3). The specific surface area (S$_{BET}$) of the MPI$_7$ sample is relatively small (~1.6 m$^2 \bullet$g^{-1}), and this value is very comparable with that
75 of the PI325 sample (1.8 m$^2 \bullet$g^{-1}), as revealed by the N$_2$ adsorption and desorption isotherms. The small BET value might be caused by the aggregation of the sample, as shown in SEM observations.
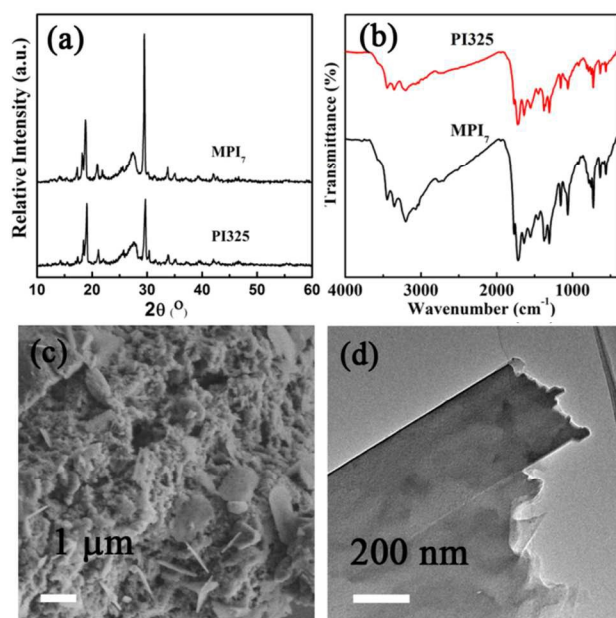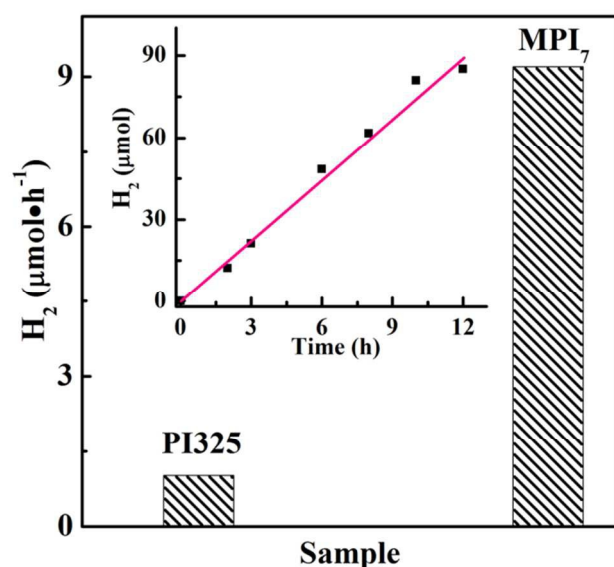

Fig. 1. Analysis of MPI$_7$, with PI325 as reference, a) XRD patterns; b)FT-IR spectra; c) SEM image and d) TEM image.

The FT-IR spectrum of MPI$_7$ is also essentially the same as that of PI325 sample (Fig. 1b). Several characteristic absorption bands
35 of C=O in polyimide at 1770, 1720, 725, and 635 cm^{-1} were observed. We also observed the stretching vibration modes of CN heterocycles (1640, 1373, 1155, and 1062 cm^{-1}).[5] The disappearance of the band at 1850 cm^{-1} of anhydride monomer

Fig. 2 The histogram showing the H_2 production rate over MPI$_7$ and PI325 sample. The H_2 production rate is taken from the first 6 h photocatalytic reaction. The inset shows the long term H_2 production over MPI$_7$ sample.

Visible-light-driven photocatalytic H_2 production was carried out using TEOA as the sacrificial electron donor.[19] 0.5 wt% Pt as co-catalyst was *in-situ* photodeposited on PI photocatalysts. Control experiments show no H_2 evolution in the absence of either PI photocatalysts or light irradiation, confirming that the hydrogen production was driven by both light irradiation and PI photocatalysts. The pristine MPI$_7$ sample shows a H_2 evolution rate of ~ 9.2 $\mu mol \cdot h^{-1}$, which is more than 9 times higher than that of the PI325 sample (~1.0 $\mu mol \cdot h^{-1}$) (Fig. 2). Note that the present PI325 sample shows lower H_2 production rate than that in reference 5. This result should be caused by the various evaluation systems for H_2 production. The pressure is below the atmospheric pressure during H_2 generation reaction in Chu's work, while the pressure in our work is greater than the atmospheric pressure. Notably, no obvious activity loss was observed after 10 h reactions, revealing the relatively excellent stability of MPI sample for photocatalytic H_2 production. The surface area is one of key factors to determine the photocatalytic H_2 production of a photocatalyst. However in present case, MPI$_7$ and PI325 sample have similar BET value (1.6 and 1.8 $m^2 \cdot g^{-1}$ for MPI7 and PI325, respectively). Therefore, the surface area difference is fairly minor as compared to the difference in H_2 evolution rate (9 times difference). Therefore, we believe that the surface area difference should not influence the photocatalytic activities for H_2 generation. Therefore, the enhanced photocatalytic H_2 production over MPI$_7$ can be attributed to the improved crystalline quality than PI325 sample, as revealed by XRD analysis (Fig. 1a). The improved crystalline quality can promote the efficient charge transfer within MPI$_7$ sample, as confirmed by photoluminescence analysis.

Steady-state photoluminescence (PL) spectra of MPI$_7$ and PI325 were measured to reveal the difference in charge behaviours in photocatalysts. As illustrated in Fig. 3a, the PI325 sample shows a strong PL emission peak at ~ 480 nm, while MPI$_7$ shows an evident red-shift PL emission peak at ~ 510 nm. The difference in

PL spectra of PI325 and MPI7 sample should be caused by the different polymerization process, as revealed by the XRD patterns and the absorption spectra. The detailed mechanism on difference in PL spectra needs further investigation. It is well known that the higher the PL intensity, the lower the photocatalytic H_2 production rate. Contrary to this expectation, the MPI$_7$ with stronger PL intensity shows higher H_2 production rate. To reveal the cause for this enhanced H_2 production rate, we carried out the ·OH radical measurement to reveal the improved separation efficient of electrons and holes in MPI$_7$. The photoexcited holes on polyimide samples can oxidize hydroxyl ions (OH$^-$) to generate ·OH radicals in the solution. It is well known that ·OH radicals can react with terephthalic acid (TA) in basic solution to generate 2-hydroxy-terephthalic acid (TAOH). The produced TAOH emit strong fluorescence signal at 426 nm.[20] Therefore, the fluorescence intensity of TAOH quantifies the number of ·OH radicals which are directly associated with the charge separation efficiency. The MPI$_7$ sample shows higher TAOH fluorescence intensity than PI325, as shown in Fig. S4. The ·OH radical measurements clearly reveal the more effective charge separation in MPI$_7$ than that in PI325, and thereby induce the high H_2 production rate.
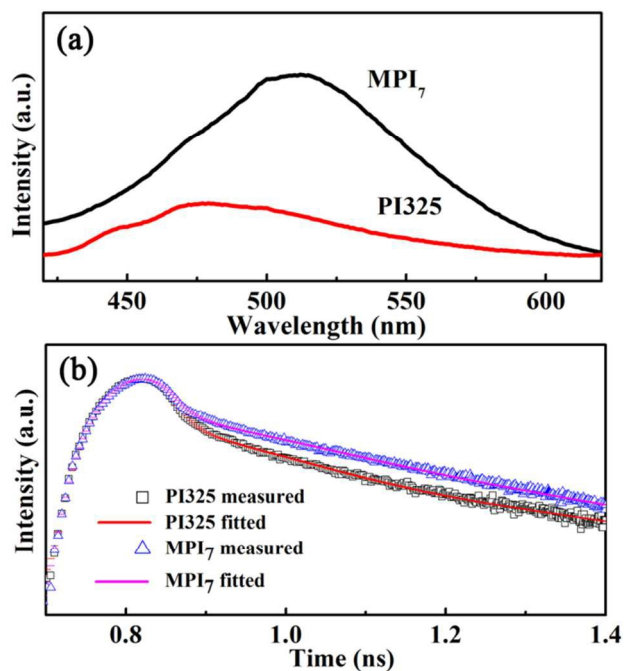
Fig. 3 (a) The stable state PL spectra and **(b)** transient fluorescence decay for MPI$_7$ and PI325, respectively.

The lifetime of the charge carriers in excited PI samples was further measured to monitor the transfer behaviours of the charge carriers using time-resolved transient fluorescence spectroscopy, as shown in Fig. 3b. The fitted lifetimes of MPI$_7$ and PI325 are listed in Table S1. MPI$_7$ sample has three radiative PL lifetime of 2.80 (weighting factor A_1=3%), 12.50 (weighting factor A_2=2%), and 0.24 ns (weighting factor A_3=95%). Comparatively, PI325 sample also has three PL lifetime of 2.32, 12.94, and 0.21 ns, respectively. Note that the A_1 increases from 3% in MPI$_7$ to 4% in PI325, while A_2 decreases from 2% in MPI$_7$ to 0% in PI325. The average PL lifetime in excited MPI$_7$ and PI325 was 0.53 and

0.34 ns, respectively. This result evidently indicates that the longer-lived charge carriers in MPI$_7$ allow the efficient photocatalytic H$_2$ production.

We further investigated the MW-reaction time on PI formation. It was found that the MW-reaction time has great effect on PI formation and on final photocatalytic H$_2$ production. Note that the XRD pattern of the products after 5 min MW-reaction is the same as that of MPI$_7$ (Fig. S5). As expected, the XRD intensity of MPI$_5$ is weaker than that of MPI$_7$. Further increasing reaction time to 10 min causes the total carbonization of the products. In addition, MPI$_5$ sample shows the same FT-IR spectrum and optical absorption behaviour with MPI$_7$ (Fig. S6 and S7), further revealing the formation of PI after only 5 min reactions. In addition, MPI5 shows 5 times higher H$_2$ production rate than PI325 (Fig. S8), further reveals the priority of present synthesis strategy.

Conclusions

We have demonstrated the rapid and green synthesis of polyimide through MW-assisted heating process. This strategy shows the following advantages over the conventional heating process. First, The reactions can be finished within 10 minutes, making the process to be time- and energy-efficient. Second, the present strategy avoids the tedious washing process or using the toxic organic reagents. Therefore, the present reaction is a green synthesis process. The last but not the least, the polyimide prepared through present strategy shows improved crystalline over the conventional heating process, resulting in the enhanced H$_2$ production. This innovative strategy provides a new route to synthesize the polyimide-related products, and can be extended to construct modified polyimide and hybrid materials based on polyimide and other semiconductors. We believe that the present process allows us to tune the chemical composition, electronic structure, and surface functionality of polyimide for catalytic reactions.

Notes and references

^{a} Laboratory of Advanced Porous Materials, School of Chemistry and Chemical Engineering, Anhui University, Hefei 230036, P. R. China A E-mail: yupengyuan@ahu.edu.cn
^{b} Innovation Lab for Clean Energy & Green Catalysis, Anhui University, Hefei 230601, P. R. China

† Electronic Supplementary Information (ESI) available: [details of any supplementary information available should be included here]. See DOI: 10.1039/b000000x/

‡ Footnotes should appear here. These might include comments relevant to but not central to the matter under discussion, limited experimental and spectral data, and crystallographic data.

1. X. Chen, S. Shen, L. Guo and S.S. Mao, *Chem. Rev.*, 2010, **110**, 6503-6570.
2. A. Kudo and Y. Miseki, *Chem. Soc. Rev.*, 2009, **38,** 253-278.
3. Y. P. Yuan, L. W.Ruan, J. Barber, S. C. J. Loo and C.Xue, *Energy. Environ. Sci.*, 2014, **7**, 3934-3951.
4. F. E. Osterloh, *Chem. Mater.*, 2008, **20**, 35-54.
5. Y. Wang, X. C. Wang and M. Antonietti, *Angew. Chem. Int. Ed.***,** 2012, **51**, 68-89.
6. S. W. Cao and J. G. Yu, *J. Phys. Chem. Lett.*, 2014, **5**, 2101-2107.
7. S. Chu, Y .Wang, Y .Guo, P. Zhou, H. Yu, L.L. Luo, F. Kong and Z.G. Zou, *J. Mater. Chem.*, 2012, **22**, 15519-15521.
8. S. Chu, Y. Wang, C.C.Wang, J.C. Yang and Z.G. Zou, *Int. J. Hydrogen Energy*, 2013, **38**, 10768-10772.
9. S. Chu, Y. Wang, Y. Guo, J.Y. Feng, C.C. Wang, W.J. Luo, X.X. Fan and Z.G. Zou, *ACS Catal.*, 2013, **3**, 912−919.
10. Y. R. Wang, S. G. Xu, T. Chen, H. W. Guo, Q. Y. Liu, B. X. Ye, Z. Zhang, Z. Q. He and S. K. Cao, *Polym.Chem.*, 2010, **1**, 1048-1055.
11. J. Weber, M. Antonietti and A. Thomas, *Macromolecules*, 2008, **41**, 2880-2885.
12. N. Ritter, M. Antonietti, A. Thomas, I. Senkovska, S. Kaskel and J. Weber, *Macromolecules*, 2009, **42**, 8017-8020.
13. J.D. Xiao, L.J. Qiu, Y.P. Yuan, X. Jiang, A.J. Xie and Y.H. Shen, *Inor. Chem. Commun.*, 2013, **29**, 128-130.
14. Y.P. Yuan, L.S.Yin, S.W. Cao, L.N. Gu, G.S. Xu, P.W. Du, H. Chai, Y.S. Liao and C. Xue, *Green Chem.*, 2014, **16**, 4663-4668
15. K. J. Rao, B. Vaidhyanathan, M. Ganguli and P. A. Ramakrishnan, *Chem. Mater.*, 1999, **11**, 882–895.
16. R. Hoogenboom and U. S. Schubert, *Macromol. Rapid Commun.*, 2007, **28**, 368-386.
17. X. C. Wang, K. Maeda, A. Thomas, K. Takanabe, G. Xin, J. M. Carlsson, K. Domen and M. Antonietti, *Nat. Mater.*, 2009, **8**, 76–80.
18 Y. Wang, X. C. Wang and M. Antonietti, *Angew. Chem., Int. Ed.*, 2012, **51**, 68–89.
19. Y.P. Yuan, W.T. Xu, L.S.Yin, S.W. Cao,Y.S. Liao, Y.Q. Tng and C. Xue, *Int. J. Hydrogen Energy*, 2013, **38**, 13159-13163.
20. Y. P. Yuan, S. W. Cao, Y. S. Liao, L. S. Yin and C. Xue, Appl. Catal. B-Environ., 2013, **140-141**, 164-168.

Polyimide was fabricated in minutes by microwave-assisted heating process. The resultant polyimide possesses high crystalline quality and shows enhanced photocatalytic H_2 generation.